Neuropsychologia 69 (2015) 218–231

Contents lists available at ScienceDirect

Neuropsychologia

journal homepage: www.elsevier.com/locate/neuropsychologia

Long-term supratentorial brain structure and cognitive function following cerebellar tumour resections in childhood

T. Moberget [a,*], S. Andersson [a,b], T. Lundar [c], B.J. Due-Tønnessen [c], A. Heldal [a,b,c,d], T. Endestad [a], L.T. Westlye [a,d]

[a] Department of Psychology, University of Oslo, Oslo, Norway
[b] Department of Psychosomatic Medicine, Oslo University Hospital, Oslo, Norway
[c] Department of Neurosurgery, Oslo University Hospital, Oslo, Norway
[d] Norwegian Centre for Mental Disorders Research (NORMENT), KG Jebsen Centre for Psychosis Research, Division of Mental Health and Addiction, Oslo University Hospital & Institute of Clinical Medicine, University of Oslo, Oslo, Norway

ARTICLE INFO

Article history:
Received 2 November 2014
Received in revised form
21 January 2015
Accepted 5 February 2015
Available online 7 February 2015

Keywords:
Cerebellum
Cognition
Development
Cerebral white matter
Cerebral grey matter

ABSTRACT

The cerebellum is connected to extensive regions of the cerebrum, and cognitive deficits following cerebellar lesions may thus be related to disrupted cerebello-cerebral connectivity. Moreover, early cerebellar lesions could affect distal brain development, effectively inducing long-term changes in brain structure and cognitive function. Here, we characterize supratentorial brain structure and cognitive function in 20 adult patients treated for cerebellar tumours in childhood (mean age at surgery: 7.1 years) and 26 matched controls. Relative to controls, patients showed reduced cognitive function and increased grey matter density in bilateral cingulum, left orbitofrontal cortex and the left hippocampus. Within the patient group, increased grey matter density in these regions was associated with decreased performance on tests of processing speed and executive function. Further, diffusion tensor imaging revealed widespread alterations in white matter microstructure in patients. While current ventricle volume (an index of previous hydrocephalus severity it patients) was associated with grey matter density and white matter microstructure in patients, this could only partially account for the observed group differences in brain structure and cognitive function. In conclusion, our results show distal effects of cerebellar lesions on cerebral integrity and wiring, likely caused by a combination of neurodegenerative processes and perturbed neurodevelopment.

1. Introduction

The cerebellum is densely connected to the cerebral cortex through heavily myelinated fibre tracts (Ramnani, 2006). However, while widespread and functionally diverse neocortical input to the cerebellum has long been acknowledged, it was until recently believed that cerebellar output was almost exclusively aimed at the primary motor cortex (Bostan et al., 2013; Ramnani, 2006). In line with this anatomical account, the functional role of the cerebellum was thought to be largely limited to motor control and coordination. Importantly, recent findings have challenged this view (Bostan et al., 2013). Transneural tracing studies in primates have demonstrated connections from the cerebellum to widespread cortical areas, including prefrontal and posterior parietal associative cortices (Kelly and Strick, 2003; Middleton and Strick, 1994; Strick et al., 2009), and results from human imaging studies are consistent with this expanding view of cerebello-cerebral connectivity (Bostan et al., 2013; Habas et al.,2013). Cerebellar and cerebral areas co-activate during the performance of a wide range of cognitive tasks (Balsters et al., 2014; Stoodley and Schmahmann, 2009) and several studies using resting state functional magnetic resonance imaging (fMRI) report functional connectivity between the cerebellum and cerebral networks involved in both cognitive functions and motor control (Bernard et al., 2014; 2012; Buckner et al., 2011; Habas et al., 2009; Krienen and Buckner, 2009; O'Reilly et al., 2010; Ramnani, 2006; Sang et al., 2012). In line with these observations, diffusion tensor imaging (DTI) based tractography has provided evidence for white-matter tracts between the dentate nucleus – a major source of cerebellar output – and prefrontal and parietal areas (Jissendi et al., 2008; Palesi et al., 2014; Ramnani, 2006), suggesting extensive structural connections between the cerebellum and the associative cerebral cortex in humans.

In light of this growing evidence for non-motor cerebello-

* Corresponding author.
E-mail address: torgeir.moberget@gmail.com (T. Moberget).

http://dx.doi.org/10.1016/j.neuropsychologia.2015.02.007
0028-3932/

cerebral networks, it has been suggested that cognitive deficits following cerebellar lesions are related to disruptions in cerebello-cerebral connectivity (Mariën et al., 2010; Miller et al., 2010). For instance, acute cerebello-cerebral diaschisis – i.e. decreased perfusion or metabolism in cerebral areas following damage to the cerebellum – has been proposed as a mechanism explaining the transient mutism that occurs in 11–29% of patients after cerebellar tumour resections (Gudrunardottir et al., 2011). Further, reduced density of cerebral grey matter has been reported in patients after focal cerebellar lesions acquired in adulthood (Clausi et al., 2009). As would be expected based on known cerebello-cerebral anatomical connections, these reductions were primarily seen contralaterally to the cerebellar lesions.

Of note, cerebellar injury in childhood generally leads to more pronounced cognitive deficits than cerebellar pathology in adults (Alexander et al., 2012; Timmann and Daum, 2010; Wang et al., 2014), with the most severe impairments seen in patients with congenital cerebellar pathology (Steinlin, 2007). It has consequently been suggested that the cerebellum plays a crucial role during neurodevelopment, and that early injury may lead to disruptions in the development of remote brain regions, a phenomenon termed *developmental diaschisis* (Wang et al., 2014). Supporting this notion, (Limperopoulos et al., 2010) reported an association between isolated pre-term cerebellar injury and reduced volumes of the contralateral cerebral cortex. Interestingly, long-term motor, cognitive and neuropsychiatric outcome in this patient group was associated with volumes of specific cerebral cortical regions (Limperopoulos et al., 2014).

Thus, it is possible that the persistent cognitive deficits reported in patients with cerebellar lesions due to tumour resections (Aarsen et al., 2004; Rønning et al., 2005; Scott et al., 2001; Steinlin et al., 2003; Vaquero et al., 2008) are also related to remote effects in supratentorial (cerebral) grey and/or white matter. While we are not aware of any studies investigating supratentorial grey matter volumes in this patient group, a few recent studies using DTI to investigate white-matter microstructural properties have reported reduced fractional anisotropy (FA) in patients treated for cerebellar medulloblastomas (Leung et al., 2004; Rueckriegel et al., 2010; Soelva et al., 2013). Further, degree of white-matter abnormalities (both volume, FA and radial diffusivity [RD]) has been shown to correlate with the severity of cognitive deficits (Brinkman et al., 2012; Khong et al., 2003; Mabbott, et al., 2006; Mulhern et al., 2001; Reddick et al., 2003). Although the craniospinal radiation therapy and chemotherapy used in the treatment of medulloblastomas may be partly responsible for these effects, reduced FA has also been found in patients with cerebellar astrocytomas, where treatment is limited to surgery (Rueckriegel et al., 2010; Soelva et al., 2013). The first aim of the present study was to compare supratentorial brain structure and cognitive function between patients with surgical resections of cerebellar tumours and matched controls, utilising advanced multimodal MRI – including voxel-based morphometry (VBM) and DTI – in combination with neuropsychological testing. Importantly, however, any observed group differences might not be directly related to the cerebellar lesion, but rather to concomitant complications such as hydrocephalus, typically occurring in about 80–90% of cerebellar astrocytoma patients (Due-Tønnessen et al., 2013; Kameda-Smith et al., 2013) due to blocking of the aqueduct by the tumour mass. This latter possibility is especially relevant with respect to white matter, as hydrocephalus may have direct neurotoxic effects on periventricular white matter (Hattori et al., 2012; Scheel et al., 2012; Yuan et al., 2013), possibly due to decreased perfusion and oedema caused by the elevated pressure (Rueckriegel et al., 2010). Studies aimed at investigating the cognitive role of the cerebellum critically rely on the assumption that resection of cerebellar tissue is the main causal factor explaining structural and cognitive outcomes. If hydrocephalus were to emerge as a more likely primary mechanism, conclusions based on these previous studies would need to be reevaluated (Aarsen et al., 2014; Omar et al., 2014).

Therefore, our second aim was to investigate possible mechanisms underlying any group differences by assessing the unique contribution of hydrocephalus severity and cerebellar lesion volumes, respectively. While we do not have data on pre-surgical hydrocephalus, previous studies have shown that ventricle volumes remain increased following hydrocephalus treatment (by tumour removal and/or shunt implants), especially for large pre-surgical volumes (Santamarta et al., 2008; St George et al., 2004). Consequently, we used current lateral ventricle volume as a putative marker of previous hydrocephalus severity and examined associations between ventricular volume and/or lesion size and measures of cognitive function and supratentorial brain structure, respectively. Finally, we explored relationships between brain structure and neuropsychological test performance. Based on the scarce previous literature and current theories about the involvement of cerebello-cerebral networks in neurodevelopment and cognitive functions, we hypothesised that focal cerebellar lesions in childhood would be associated with long-term cognitive deficits and abnormalities in supratentorial brain structure.

2. Materials and methods

2.1. Participants

Table 1 summarizes demographic information on the participants. Twenty-eight patients who had undergone surgical resections of low-grade cerebellar tumours (pilocytic astrocytomas) were initially recruited from the Department of Neurosurgery and the Department of Psychosomatic Medicine at Oslo University Hospital. Eight patients were excluded from the final sample: two due to metal implants precluding MRI, one because of extensive extra-cerebellar lesions and an estimated IQ below 70, two because of extra-cerebellar lesions to the brainstem, one due to having received additional radiation treatment, one due to excessive imaging artifacts caused by a metal implant and one because age at surgery (34 years) was a clear outlier relative to the rest of the group (range from 0 to 14 years). Of the remaining 20 patients (age range: 16–30 years), five had at some point been treated for post-surgical hydrocephalus with shunt-implants. Mean age at surgery was 7.1 years (SD: 4.1), while mean time since surgery at testing was 12.9 years (SD: 4.3; range: 5–22). Symptoms of cerebellar ataxia were quantified by a neurologist and/or neurosurgeon (T.L. & B.D-T) using the Scale for Assessment and Rating of Ataxia (SARA, (Schmitz-Hübsch et al., 2006, which has a total score ranging from 0 to 40. Patients (N = 18, as ratings were

Table 1
Group demographic characteristics.

Measure	Patients (N=20)	Controls (N=26)	Effect size[a]	p-Value[b]
Sex [% female]	40	50	.100	.500
Age [years: mean (SD)]	20.0 (4.0)	21.0 (5.1)	.22	.453
Handedness [% left]	20.0	11.5	.117	.428
Education [years: mean (SD)]	11.5 (1.1)	12.9 (2.1)	.82	**.004**

[a] For categorical variables, we give Fisher's *Phi*, while for continuous variables Cohen's *d* is used.

[b] p-Values are based on chi-square tests for categorical variables and on independent samples t-tests (two-tailed) for continuous variables. $ps < .05$ are marked in bold.

missing from two patients) had a mean total SARA-score of 2.67 (SD: 3.50), with a range from 0 to 12, indicating minimal to moderate ataxia symptoms in the current sample. Six included patients fulfilled diagnostic criteria for one or more current (four patients) or previous (two patients) ICD-10 psychiatric diagnoses (within the domain of anxiety and mood disorders), as determined by the MINI Neuropsychiatric Interview (Sheehan et al., 1998) conducted by an experienced psychiatrist (A.H).

Twenty-eight age- and sex-matched healthy control participants (age range: 16–33 years) were recruited from the local community. Control participants reported no neurological or current psychiatric problems. Two control participants were excluded due to brain abnormalities discovered during the neuroradiological examination.

The study was approved by the Regional Ethics Committee of Southern Norway (REK-Sør), and written informed consent was acquired from all participants. For participants younger than 18, written informed consent was also acquired from a parent.

2.2. Cognitive testing

All participants completed a battery of neuropsychological tests lasting approximately one and a half hours. Vocabulary and Matrix Reasoning subscales of Wechsler Abbreviated Scale of Intelligence (WASI) were used to assess general cognitive abilities; i.e., estimated IQ (Wechsler, 1999). In addition, we tested processing speed (Colour Naming and Reading parts of the Color-Word Interference Test from the D-KEFS battery (Delis et al., 2001), working memory (Digit Span and Letter Number Sequencing, from WAIS-III (Wechsler, 1997), executive functions (Inhibition and Inhibition/Switching parts of the Color Word Interference Test from the D-KEFS, Verbal Fluency from D-KEFS), and verbal (California Verbal Learning Test - II, (Delis et al., 2000) and visual (Brief Visuospatial Memory Test – Revised, (Benedict, 1997) learning and memory. With the exception of estimated IQ we report raw test scores. Summary scores for each cognitive domain were computed by transforming raw data to *z*-scores and averaging these within each domain.

All statistical analyses of neuropsychological test scores were conducted using SPSS 21 (SPSS, Chicago, IL, USA) and a two-tailed p-value $< .05$ was considered statistically significant. For estimated IQ, group differences were examined with independent samples *t*-test. All other test scores were examined using analyses of covariance (ANCOVAs) with sex and group as fixed factors, and age and handedness as covariates.

2.3. Image acquisition

Imaging was performed with a Philips Achieva 3 T whole body MR unit equipped with an 8-channel Philips SENSE head coil (Philips Medical Systems, Best, the Netherlands). For lesion reconstruction, voxel based morphometry and quantification of lateral ventricle volumes we acquired high-resolution T1-weighted (180 sagittal slices; TR: 8.5 ms; TE: 2.3 ms; voxel size 1.0x1.0x1 mm^3, FOV: 256x256x180; flip angle: 7°) and T2-weighted fluid attenuated inversion recovery (FLAIR) (150 sagittal slices; TR: 8.0 ms; TE: 330.5 ms; inversion time: 2400 ms; voxel size 1.0x1.0x1.2 mm^3, FOV: 256x256x180; flip angle: 90°) sequences. For DTI, a single-shot twice-refocused spin-echo echo-planar imaging sequence was used: repetition time (TR)/echo time (TE) = 10,660 ms/53 ms, maximum *b*-value = 1000 s/mm^2, voxel size = 2.0x2.0x2.0 mm^3, and 60 axial slices. The sequence consisted of 1 $b=0$ and 32 diffusion-weighted volumes collected along 32 non-collinear directions.

2.4. Lesion reconstruction

Cerebellar lesions were manually drawn on the T1-weighted volume using MRICron (Rorden et al., 2007). FLAIR volumes were used to correct the T1-based lesion maps when the former indicated more extensive tissue damage. A neurologist with extensive experience in lesion-mapping examined all reconstructed lesions. We subsequently used the SUIT-toolbox (Diedrichsen, 2006) in SPM8 (http://www.fil.ion.ucl.ac.uk/spm/software/spm8) to normalise all lesion maps into common space. Lesion volumes were calculated from these normalised images, thus adjusting for individual differences in total cerebellar volume. MRIcron (Rorden et al., 2007) was used to compute lesion overlap maps, while information about affected cerebellar lobules and nuclei were extracted from a probabilistic cerebellar atlas in the SUIT-toolbox (Diedrichsen, 2006).

2.5. Voxel-based morphometry and volumetric segmentation

For voxel-based morphometry, we first realigned and resampled the FLAIR-images to the T1-images in SPM8. Next, both T1 and FLAIR images were used in multi-spectral tissue segmentation using the New Segment toolbox in SPM8. Following the procedure of (Seghier et al., 2008), we included an extra tissue probability map (the mean of the white matter and CSF maps) as an additional prior in this segmentation step in order to prevent lesioned brain tissue from being erroneously classified as grey matter. This extra prior was iteratively refined by thresholding the voxels assigned to this class at .33 and using this pruned image as the tissue class prior in the next step. Two iterations were performed. Inspection of the tissue segmentations confirmed that inclusion of the FLAIR scans significantly improved the quality (primarily by preventing dura and blood vessels from being classified as grey matter) and that the extra tissue prior had the intended effect of isolating lesioned tissue. Grey matter segmentations were subsequently normalised to MNI-space using the high-dimensional nonlinear diffeomorphic anatomical registration tool DARTEL (Ashburner, 2007). Since Jacobian modulation, i.e. the multiplication of normalised grey matter maps by the Jacobian of the transformation matrix in order to preserve local grey matter volume, is likely to affect the results (Eckert et al., 2006; Henley et al., 2010), we tested both unmodulated and modulated maps in order to facilitate the comparison with previous and future studies. In line with common terminology we refer to unmodulated maps as grey matter density and modulated maps as grey matter volume. Normalised grey matter maps (resampled to $1.5 \times 1.5 \times 1.5$ mm^3 voxel size) were smoothed with an 8 mm FWHM Gaussian kernel and subjected to group-level statistical analyses using nonparametric permutation testing (Winkler et al., 2014) as implemented in randomise, part of the Oxford Centre for Functional MRI of the Brain (FMRIB) Software Library (FSL) (Smith et al., 2004). Voxels were included if they overlapped a mask created by thresholding the mean of the (unsmoothed) normalised grey matter maps at 0.1. We tested for main effects of group (patients, controls) by means of general linear models (GLMs) while covarying for sex, age and handedness. Threshold Free Cluster Enhancement (TFCE) (Smith and Nichols, 2009) was used for statistical inference, with 10,000 permutations performed for each contrast. Statistical maps were thresholded at $p < 0.05$ (two-tailed, corrected for multiple comparisons across space). In order to estimate effect sizes (Cohen, 1992) and test possible associations between structural indices and cerebellar lesion volume, ventricle volume and the cognitive domain scores we extracted the mean values across voxels showing significant group effects for further analysis in SPSS.

Total brain volume was calculated by summing the volumes of

the grey matter, white matter, CSF and the extra tissue class segmentations (Ridgway et al., 2011). Lateral ventricle volumes were calculated from CSF-segmentations using the ALVIN toolbox (Kempton et al., 2011).

2.6. Diffusion tensor imaging (DTI)

DTI datasets were processed using FSL (Smith et al., 2004). Each volume was affine registered to the first $b=0$ volume using FMRIB's Linear Image Registration Tool (Jenkinson et al., 2002) to correct for subject motion and eddy currents. Since in-scanner subject motion can affect group differences in DTI indices (Yendiki et al., 2014), we included estimates of individual mean relative motion in subsequent analyses.

After removal of nonbrain tissue (Smith, 2002), FA (Basser and Pierpaoli, 1996), eigenvector, and eigenvalue maps were computed by linearly fitting a diffusion tensor to the data. We defined RD as the mean of the second and third eigenvalue $[(\lambda 2+\lambda 3)/2]$ and mean diffusion (MD) as the mean of all three eigenvalues. FA volumes were skeletonised and transformed into common space using tract-based spatial statistics (TBSS) (Smith et al., 2006) All volumes were nonlinearly warped to the FMRIB58_FA template using local deformation procedures performed by FMRIB's Nonlinear Image Registration Tool. Next, a mean FA volume across all subjects was generated and thinned to create a mean FA skeleton representing the centres of common tracts, including superior aspects of the brainstem and cerebellum. We thresholded and binarized the mean skeleton at FA >0.25. Similar warping and analyses were used for axial diffusion (AD), RD, and MD data.

Voxel-wise analyses were performed using nonparametric permutation testing (Winkler et al., 2014). We tested for main effects of group (patients, controls) by means of GLMs while covarying for sex, age and handedness. TFCE (Smith and Nichols, 2009) was used for statistical inference, with 10,000 permutations performed for each contrast. Statistical maps were thresholded at $p<.05$ (two-tailed, corrected). DTI values averaged across voxels showing significant group effects were used in univariate ANCOVAs to estimate frequently reported effect sizes (Cohen, 1992) and to assess the effects of possible confounding variables, such as estimated subject motion during scan acquisition, IQ and ventricle volume.

2.7. Analyses of effects of cerebellar lesion volume and ventricle volume

In order to explore possible mechanisms in the cerebellar patient group, we first examined effects on cognitive function in a multivariate analysis of covariance (MANCOVA) in SPSS including the five cognitive domain scores as dependant variables, sex as a fixed factor and cerebellar lesion volume, ventricle volume and age as covariates. Effects on grey matter density and DTI-indices were investigated in a set of univariate ANCOVAs with the structural brain index (averaged across voxels showing a significant effect of group) as the dependent variable, sex as a fixed factor and lesion size, lateral ventricle volume and age as covariates.

2.8. Exploratory analyses of structure-structure and structure-function relationships

Associations between grey and white matter indices were explored using Spearman correlation analyses. Relationships between brain structure indices and the five cognitive domain scores were explored in a set of MANCOVAs with the cognitive domain scores as dependent variables, sex as a fixed factor and the structural index and age as covariates.

3. Results

3.1 Lesion reconstruction

Fig. 1 gives an overview of affected lobules and nuclei in individual patients and lesion overlap for the group. The mean volume of cerebellar resections was 19.9 ml (SD: 15.0), ranging from 4.36 ml to 53.03 ml. Lesions primarily affected the vermis, while the fastigial and interposed were the most affected deep cerebellar nuclei.

3.2. Neuropsychological performance

Table 2 summarizes estimated IQ and neuropsychological scores for cerebellar patients and controls.

Compared to age- and sex-matched controls, cerebellar patients showed significantly reduced performance across several tests and domains, with medium to large effect sizes (Cohen, 1992). The modest – but significant – group difference in estimated IQ is in line with a large study of 103 patients treated for cerebellar astrocytomas (Beebe, 2005). However, since we cannot exclude the possibility that our recruited control group was not adequately matched in terms of general cognitive function, we performed additional analyses covarying for IQ. In these more conservative analyses, significant group differences still remained on most measures (marked with an asterisk in Table 2). Including years of completed education as a covariate had minimal effects of the results. Given the presence of current or previous psychiatric comorbidity in 30% of the patient sample and reliable findings of modest cognitive deficits in depression (Rock et al., 2013) and anxiety disorders (Castaneda et al., 2008), we finally reran these analyses using only the 14 patients with no lifetime history of ICD-10 diagnosis. Using this smaller sample, group differences on most measures remained robust (marked with a plus sign in Table 2), but group effects on working memory indices, CWIT reading speed and CWIT inhibition were no longer significant (most showed trend effects) while phonetic fluency now showed a significant group effect.

3.3. Volumetry

Table 3 summarizes the results from the global volumetric analyses. Grey matter, white matter and total brain volume did not differ between groups, but patients showed enlarged lateral ventricles relative to controls. Lateral ventricle volume was moderately correlated with cerebellar lesion volume (Spearman's rho=.45, $p=.047$).

3.4. Voxel-based morphometry (VBM)

Fig. 2 and Table 4 display results from the VBM analyses. As expected, patients showed reduced grey matter density (based on unmodulated VBM maps) and volume (based on modulated VBM maps) in midline cerebellum. Further, we observed significantly increased grey matter density for patients relative to controls in bilateral cingulate cortices, left orbitofrontal cortex and left hippocampus. Uncorrected statistical maps (Supplementary Fig. 1) suggested widespread density and volume increases in the patient group, and except for the clusters centred in the cerebellum no regions with decreases were observed, even at the uncorrected level.

ANCOVA with mean grey matter density value across significant cerebral voxels as the dependent variable, sex and group as fixed factors, and age as a covariate revealed a significant effect of group ($F(1,41)=41.229$, $p<.000001$), as expected. Including IQ and ventricle volume as additional covariates yielded no effect of

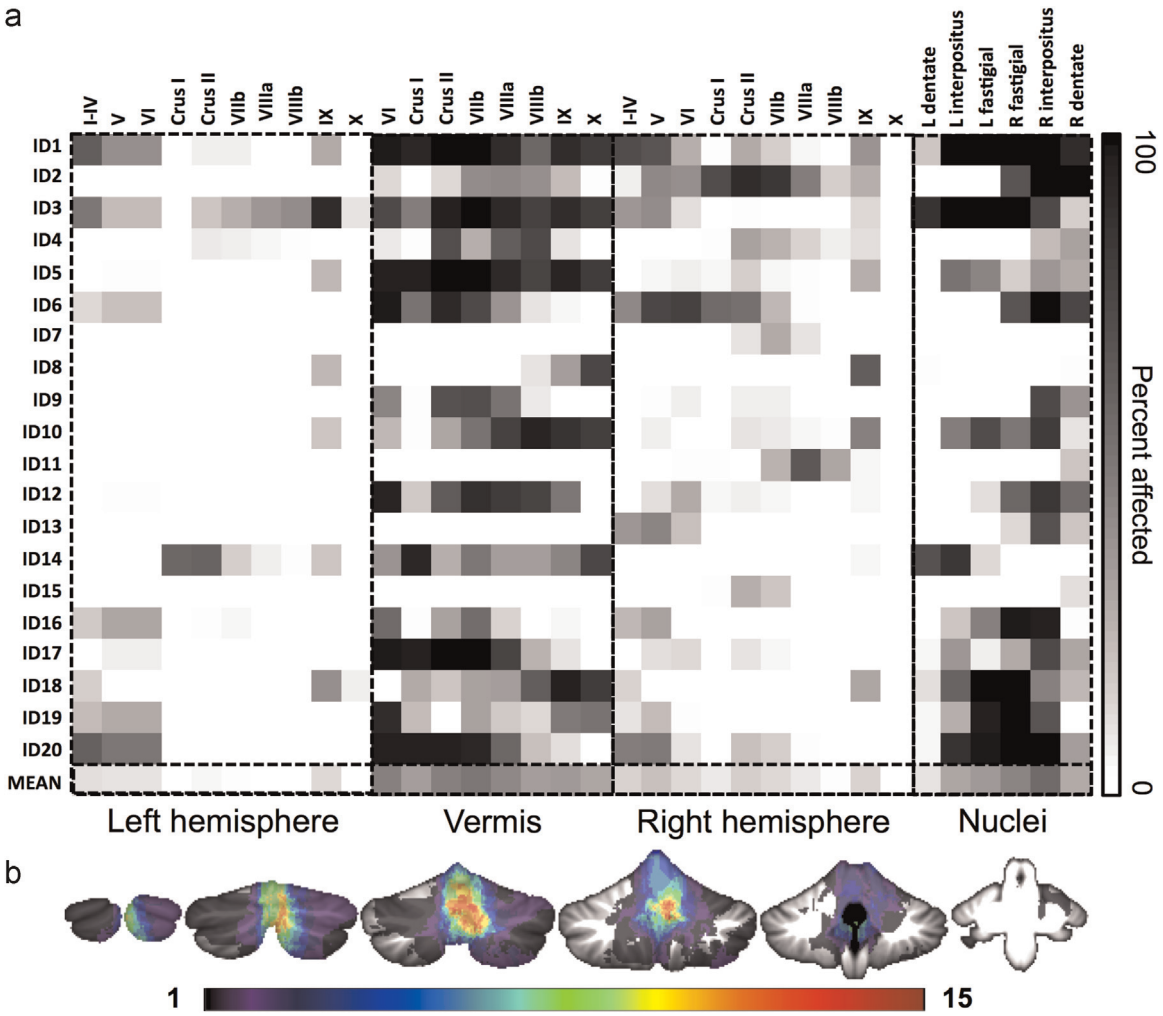

Fig. 1. (a) The fraction of cerebellar lobules and nuclei (columns) affected by the lesions in individual patients (rows) and mean affection of each region across all patients (bottom row). Label assignment is based on the probabilistic cerebellar atlas in the SUIT-toolbox (Diedrichsen, 2006). (b) Overlap of cerebellar lesions displayed on coronal sections of the SUIT template (Diedrichsen, 2006). The colorbar indicates the number of patients with lesions at a particular voxel. (For interpretation of the references to colour in this figure legend, the reader is referred to the web version of this article.)

IQ, but ventricle volume showed a significant positive association with grey matter density across groups (see further results within the patient group below). Importantly, the group effect remained significant ($F(1,39)=27.614$, $p=.000006$) with these additional covariates included. Since grey matter changes are also seen in depression (Bora et al., 2012) and anxiety disorders (Shang et al., 2014), we performed a final control analysis restricted to the 14 patients without current or precious psychiatric comorbidity and the control group. Here, the group difference remained significant ($F(1,35)=33.794$, $p=.000001$), also when including IQ and ventricle volume as covariates ($F(1,33)=16.849$, $p=.000250$).

3.5. Diffusion tensor imaging (DTI)

Fig. 3 depicts the main results from the DTI analyses. Anatomically widespread group effects were observed for all DTI-indices, indicating decreased FA and increased MD, AD and RD in patients relative to controls.

For mean FA across significant voxels, the post hoc GLM with sex and group as fixed variables and age as a covariate revealed a significant effect of age ($F(1,41) = 15.445$, $p=.000319$), sex ($F(1,41)=8.898$, $p=.005$), and group ($F(1,41)=54.253$, $p < .000001$). FA decreased with increasing age ($t=-3.930$), was higher in males than in females ($t=2.628$) and was reduced in patients relative to controls ($t=-4.814$). For MD, we observed significant effects of group ($F(1,41)=64.488$, $p < .000001$) and age ($F(1,41)=8.420$, $p=.006$). MD was increased in patients relative to controls ($t=5.803$) and increased with age ($t=2.902$). For AD, the GLM revealed a significant effect of group ($F(1,41)=68.239$, $p < .000001$), with increased AD in patients relative to controls ($t=5.824$). For RD, we observed significant effects of age ($F(1,41)=11.565$, $p=.002$) and group ($F(1,41)=59.264$, $p < .000001$). RD increased with age ($t=3.401$) and was increased in patients relative to controls ($t=5.461$).

Mean relative in-scanner subject motion did not differ between patients and controls ($t=.849$, $p=.400$), and including this as an additional covariate in the models did not markedly affect any of the DTI results. Given the significant group differences in IQ and ventricle volume, we also reran all analyses with these variables as additional covariates. While ventricle volume accounted for some of the variation in DTI-indices (see further results within the patient group below), we observed no significant effects of IQ. Importantly, all group effects remained significant (all F-values >29.854, all p-Values $<.000005$). Since changes in DTI-indices are also seen in depression (Liao et al., 2013) and anxiety disorders (Ayling et al., 2012; Daniels et al., 2013), we performed a final set of control analyses restricted to the 14 patients without current or precious psychiatric comorbidity and the control group. In these,

Table 2
Means (SDs) and effect sizes for estimated IQ and cognitive test scores.

Measure	Patients ($N=20$)	Controls ($N=26$)	Effect size[a]	p-Value[b]
IQ	95.2 (8.6)	106.9 (10.8)	1.07	**.001**+
Vocabulary	50.4 (7.2)	58.9 (7.2)	1.09	**.001**+
Matrix reasoning	25.4 (3.3)	27.8 (4.4)	.54	.095
Working memory	−.45 (.60)	.35 (.95)	.90	**.007***
Digit span	12.7 (2.7)	15.8 (4.4)	.74	**.024**
Letter-number sequencing	9.1 (1.9)	11.3 (2.8)	.85	**.010***
Processing speed	−.51 (1.1)	.39 (.51)	1.03	**.002***+
CWIT – Naming	33.9 (7.4)	28.0 (4.2)	.94	**.005***+
CWIT – Reading	26.6 (8.3)	20.7 (3.0)	.94	**.005***
Executive functions	−.33 (.84)	.25 (.62)	.73	**.026**+
CWIT – Inhibition[c]	62.8 (22.2)	50.8 (12.5)	.66	**.041**
CWIT – Inhibition/switching[c]	71.4 (23.6)	54.2 (9.5)	1.11	**.001***+
Word fluency – Phonetic FAS	38.0 (12.7)	45.1 (11.2)	.45	.163+
Word fluency – Categories	45.8 (11.1)	49.8 (10.8)	.24	.606
Word fluency – Switching	13.5 (2.9)	14.7 (3.0)	.26	.408
Verbal learning and memory	−.58 (.91)	.45 (.70)	1.5	<**.00005***+
CVLT – Learning	51.2 (8.0)	61.5 (6.6)	1.62	<**.00001***+
CVLT – Delayed recall[c]	11.7 (2.6)	13.9 (2.0)	1.03	**.002***+
Visual learning and memory	−.48 (1.1)	.37 (.72)	0.95	**.004***+
BVMT – Learning	22.7 (7.3)	28.5 (5.1)	.93	**.005***+
BVMT – Delayed recall[c]	9.4 (2.3)	11.2 (1.6)	.74	**.022**+

[a] Cohen's *d*.
[b] The *p*-Value and effect size for estimated IQ is based on an independent samples *t*-test (two-tailed). For all other measures, *p*-Values and effect sizes are based on GLMs with group and sex as fixed factors and age and handedness as covariates. *ps* $<.05$ are marked in bold. *ps* marked with an asterisk (*) remained significant in GLMs including full-scale IQ as an additional covariate, while a plus sign (+) denotes significant ($p<.05$) group effects in analyses restricted to controls and the 14 patients without any psychiatric co-morbidity.
[c] *p*-Values and effect sizes are based on ANCOVAs using log-transformed dependent variables since the assumption of normally distributed residuals was violated in ANCOVAs using the original values.

all group effects remained significant (initial analyses: all *F*-values (1, 35) >56.849, all *p*-Values $<.000001$; with IQ and ventricle volume included: all *F*-values (1,33) >27.801, all *p*-Values $<.000009$).

3.6. Effects of cerebellar lesion volume and ventricle size in patients

MANCOVA with summary scores from the cognitive domains as dependent variables, sex as a fixed factor and cerebellar lesion volume, ventricle volume and age as covariates did not yield any significant effects. Results from the analyses of structural brain indices are given in Table 5.

Larger ventricle volumes were associated with increased grey matter density, AD, MD and RD, and showed a trend association with decreased FA. Cerebellar lesion volume showed a significant positive association with RD.

3.7. Exploratory analyses of structure-structure and structure-function relationships

Using the structural indices averaged across voxels showing main effects of group, Spearman correlation analyses revealed significant associations between grey matter density and FA ($rho=-.550$, $p=.012$), MD ($rho=.586$, $p=.007$), AD ($rho=.484$, $p=.031$) and RD ($rho=.609$, $p=.004$) in the patient group. No significant correlations were observed in the control group (all *rho*-values $<\pm.186$, all *p*-Values $>.364$).

MANCOVA exploring associations between grey matter density and the five cognitive domain scores in the patient group yielded a significant overall effect of grey matter density (Wilks' Lambda (5,12)=.314, $F(5,12)=5.242$, $p=.009$). Follow-up ANOVAs revealed that this was driven by associations with processing speed ($F(1,16)=11.565$, $t=-3.401$, $p=.004$) and executive function ($F(1,16)=6.196$, $t=-2.489$, $p=.024$). Fig. 4 displays scatterplots showing the correlations between grey matter density and these cognitive domain scores.

MANCOVAs exploring associations between DTI-indices and cognitive function did not yield any significant results.

Table 3
Means (SDs) and effect sizes for volumetric measures.

Volumetric index	Patients ($N=20$)	Controls ($N=26$)	Effect size[a]	p-Value[b]
Total brain (ml)	1618.67 (159.97)	1584.95 (139.48)	.13	.688
Grey matter (ml)	737.46 (76.12)	717.31 (68.22)	.17	.580
White matter (ml)	517.97 (54.19)	503.95 (48.57)	.21	.510
Lateral ventricles (ml)	25.47 (14.06)	17.49 (5.28)	.66	**.025**

p-Values and effect sizes are based on ANCOVAs using log-transformed dependent variables as the assumption of equal error variances was violated for the original values.
[a] Cohen's *d*, calculated from the estimated marginal means and mean square error of the GLMs.
[b] *p*-Values and effect sizes are based on GLMs with group and sex as fixed factors and age as a covariate. *ps* $<.05$ are marked in bold.

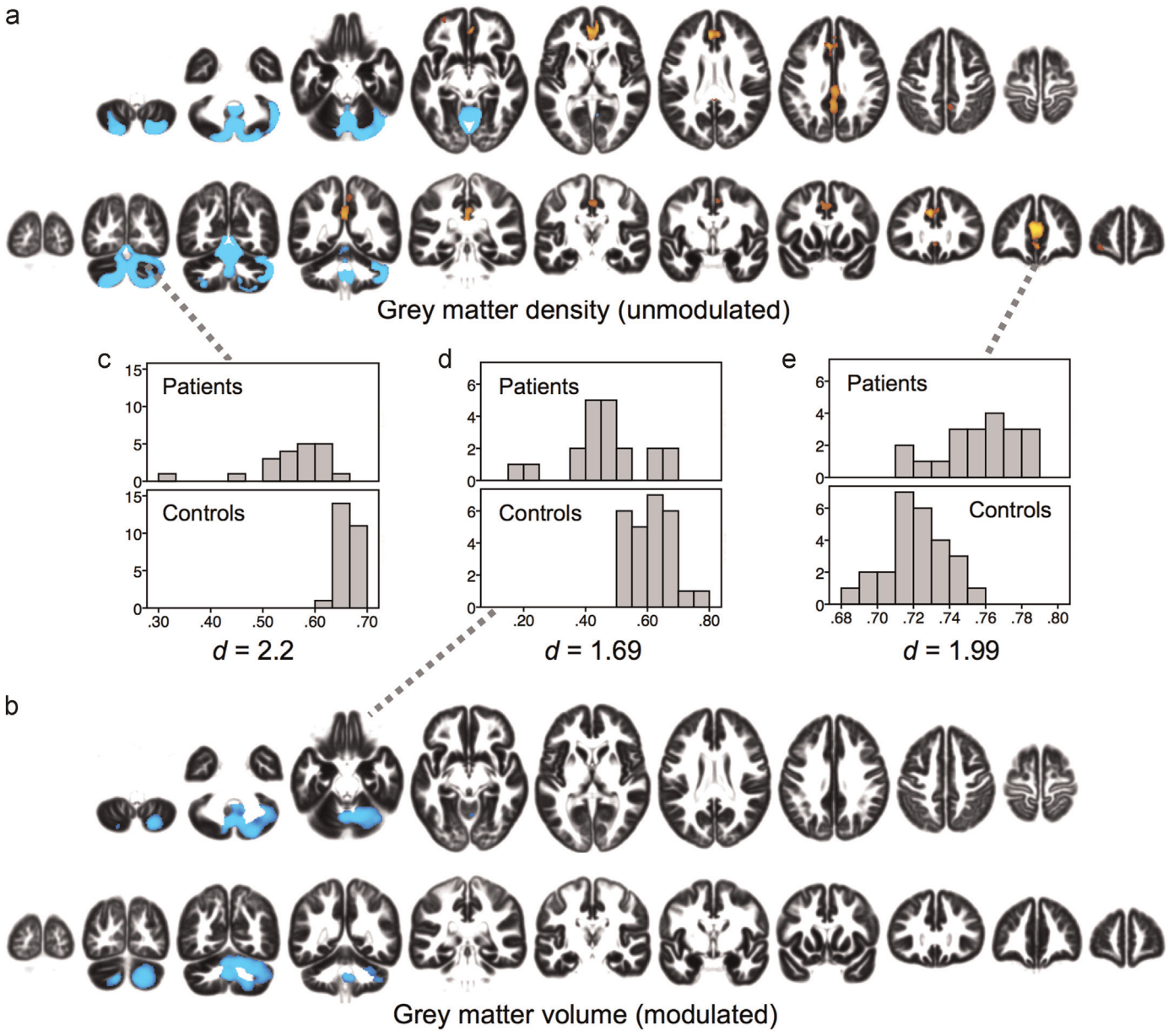

Fig. 2. Areas of significantly decreased grey matter density (a) and volume (b) in patients relative to controls is shown in cyan, while areas of significantly increased grey matter density/volume in patients relative to controls are shown in red/yellow. Group differences are thresholded at $p < .05$ (two-sided) after permutation testing using threshold free cluster enhancement (TFCE), and displayed according to the neurological convention on axial and coronal sections of the mean grey matter segmentations. Histograms (c–e) display the distributions of mean grey matter density and volume values (averaged across significant voxels). Cohen's *d* was calculated as a measure of effect size from the estimated marginal means and mean square error of GLMs with group and sex as fixed factors and age as a covariate. (For interpretation of the references to colour in this figure legend, the reader is referred to the web version of this article.)

4. Discussion

The primary aim of the present study was to conduct a comprehensive examination of supratentorial brain structure and cognitive function in patients with surgical resections of cerebellar tumours. Our secondary aim was to investigate possible mechanisms by testing the effects of lesion size and ventricular volume (as an indirect marker of previous hydrocephalus severity) on indices of brain structure and function showing significant group effects.

4.1. Main results in relation to previous findings

We observed moderately reduced cognitive function in cerebellar tumour patients relative to controls, with the most pronounced differences on tests of verbal working memory, processing speed and verbal and visual learning and memory. These findings are largely consistent with previous studies of cognitive function in this patient group (Beebe, 2005; Rønning et al., 2005), but stand in some contrast to findings in patients with cerebellar lesions acquired in adulthood, where cognitive deficits – when present – tend to be more subtle (Alexander et al., 2012). Given that the mean age at surgery in the present group was 7.1 years, our results add to the growing literature demonstrating more pronounced cognitive effects with earlier lesions and thus suggesting an important role for the cerebellum in cognitive development (Alexander et al., 2012; Timmann and Daum, 2010). Of note, reduced performance on most cognitive tests was also seen when restricting the analyses to patients without any current or previous psychiatric co-morbidity. While cognitive functions have most consistently been associated with the lateral

Table 4
Grey matter density clusters showing significant group effects.

Contrast	Volume	Coordinates			*p*-Value	Anatomical
	(mm^3)	*x*	*y*	*z*	(corr.)	labels
Patients > controls	14016.4	−1.5	42	13.5	.0023	**L anterior cingulum (24%)**, R middle cingulum (17%), L middle cingulum (15%), R anterior cingulum (11%), L posterior cingulum (6%), L superior frontal gyrus: medial (5%), R precuneus (5%), R middle frontal gyrus: orbital (3%), L precuneus (3%), R superior frontal gyrus: medial (2%), R supplementary motor area (1%), L supplementary motor area (1%), R posterior cingulum (1%), L middle frontal gyrus: medial orbital (< 1%), L olfactory cortex, (< 1%), R olfactory cortex. (< 1%).
	195.75	−30	57	−9	.0214	**L middle frontal gyrus: orbital (97%)**, L superior frontal gyrus: orbital (3%).
	94.5	−15	−30	−6	.0244	**L hippocampus (50%)**, L lingual gyrus (4%).
	47.25	−21	−36	0	.0234	**L hippocampus (93%)**.
Controls > patients	68590.13	−12	−82.5	−45	.0001	**Cerebellum (82%),** R lingual gyrus (3%), L lingual gyrus (2%), R fusiform gyrus (< 1%), R inferior temporal gyrus (< 1%), L calcarine sulcus (< 1%), R inferior occipital gyrus (< 1%).
	91.13	−24	−70.5	−33	.0248	**L cerebellum (100%).**

We present the volume of the cluster and MNI coordinates of the lowest *p*-Values within each cluster. Probabilistic anatomical labels are taken from the AAL atlas for SPM (Tzourio-Mazoyer et al., 2002) Percentages in parentheses denote the fraction of voxels in the cluster assigned to that probabilistic label. Anatomical labels in bold font correspond to the MNI-coordinates of minimal cluster *p*-Values.

cerebellar hemispheres (E et al., 2014; Stoodley and Schmahmann, 2009), which were less affected in the current patient sample, we note that activations related to working memory and executive functions have also been reported in midline cerebellar regions (E et al., 2014), and that the posterior vermis shows functional connectivity with cerebral areas associated with higher cognitive functions (Sang et al., 2012; Bernard et al., 2012).

In addition to the neuropsychological effects, we observed several differences in supratentorial brain structure between patients and controls. Specifically, increased grey matter density in bilateral cingulate, left orbitofrontal cortex and left hippocampus was found in patients relative to controls. Further, widespread white matter microstructural differences were observed, indicating reduced FA, and increased MD, RD and AD in patients. Whereas further studies are needed, the significant correlation between grey matter density and DTI-indices within the patient group suggests some common mechanisms accounting for the grey and white matter changes.

The current white matter findings are consistent with previous reports of reduced supratentorial FA in cerebellar tumour patients (Rueckriegel et al., 2010; Soelva et al., 2013), and widespread changes in extra-cerebellar white matter thus appears to be a robust and replicable finding in this patient group, even when treatment is limited to surgical intervention, avoiding the known risk associated with radiation therapy (Hoang et al., 2014; Uh et al., 2013) and the possible risk associated with chemotherapy (Simó et al., 2013). While we are not aware of other studies investigating supratentorial grey matter following cerebellar tumour surgery, our results stand in marked contrast to reports of decreased cerebral grey matter volume following cerebellar injury in infancy (Bolduc et al., 2011; Limperopoulos et al., 2010; 2014; 2005) and decreased grey matter density following lesions acquired in adulthood (Clausi et al., 2009). Taken together, these findings suggest that long term effect on cerebral structures may depend on the developmental stage at cerebellar injury, in line with the notion of sensitive periods for brain development (Wang et al., 2014).

Notably, the developing cerebral cortex shows an initial growth in early childhood (Lyall et al., *in press*), followed by a subsequent decrease. This inverted U-shape is evident in both grey matter density and grey matter volume (Taki et al., 2013), cortical thickness (Lyall et al., *in press;* Shaw et al., 2008; Tamnes et al., 2013) and surface area (Fjell et al., 2015; Wierenga et al., 2014) measures, with different peak ages for these respective measures ranging from about 2 years for cortical thickness (Lyall et al., *in press*) to about 8–12 years for cortical surface area (Brown et al., 2012; Wierenga et al., 2014). While the mechanisms underlying these developmental trajectories remain unclear, they likely involve at least an initial increase in the number of neurons and synapses per neuron, and a subsequent decrease in the number of synapses as well as an increase of cortical myelination during adolescence and young adulthood (Taki et al., 2013).

It is increasingly appreciated that brain development is activity dependent (Hensch, 2005) and losing the neural input from the cerebellum could thus potentially affect all these mechanisms of cortical development, with lesions in infancy impacting the initial growth and lesions in later childhood or adolescence impacting the subsequent synaptic pruning and/or cortical myelination. Importantly, however, the dynamic neurodevelopmental changes reviewed above also implicate that age at testing is critical for the interpretation of the results. Indeed, a recent study (Schnack et al., *in press*) found that while higher intelligence was associated with a thinner cerebral cortex at age 10, this relationship inverted over development so that by age 42 the more commonly reported positive association between cortical thickness and cognitive function was seen. In line with these findings, which strongly supports a dynamic lifespan perspective when interpreting brain-behaviour associations, decreased cerebral grey matter volume and density in infant patients may reflect perturbed neurodevelopmental mechanisms which could later manifest as increases in young adulthood and eventually as decreased volumes and density in follow-up studies of the same patients. Longitudinal studies of the same patient cohorts are needed to address these questions.

As an alternative to developmental effects, the different aetiology – and especially the presence of hydrocephalus in the present patient group – could potentially account for this discrepancy with previous findings. We address this question in the section on possible mechanisms.

The grey matter density effects were most prominent in the bilateral cingulate cortices, with significant clusters also seen in the left orbitofrontal cortex and left hippocampus. Interestingly, recent tract tracing studies in rodents demonstrate dense connections from the cingulate (Galgiani, 2013; Suzuki et al., 2012) and orbitofrontal (Suzuki et al., 2012) cortex to the posterior vermis of the cerebellum, the cerebellar region most affected in the current patient group. With respect to the hippocampus, projections from the cerebellar fastigial nuclei to the hippocampus have been known for some time (Heath and Harper, 1974), and

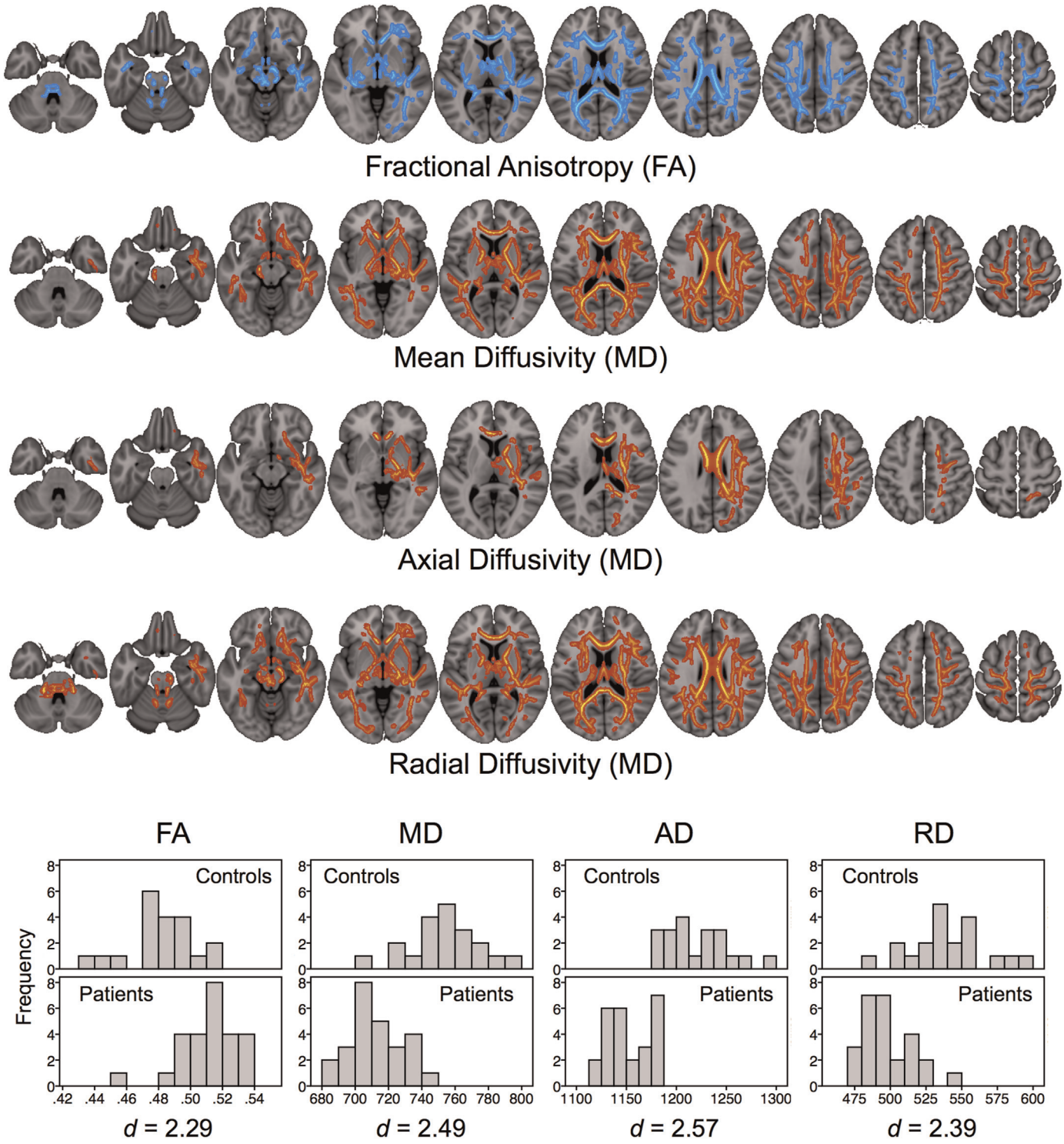

Fig. 3. Coloured voxels show significantly decreased (blue) and increased (red) DTI-indices in cerebellar patients relative to sex- and age-matched controls. Group differences are thresholded at $p < .05$ (two-tailed) after permutation testing using threshold free cluster enhancement (TFCE). Note that the white matter skeleton has been slightly thickened to aid visualisation and that images are displayed according to the neurological convention. Histograms display the distributions of mean DTI-values (averaged across significant voxels). MD, AD and RD indices have been multiplied by 10^6 in order to preserve precision. Cohen's *d* was calculated as a measure of effect size from the estimated marginal means and mean square error of GLMs with group and sex as fixed factors and age as a covariate. (For interpretation of the references to colour in this figure legend, the reader is referred to the web version of this article.)

electrophysiological responses in the hippocampus have also been recorded following fastigial and vermal stimulation in monkeys and cats (Heath et al.,1978; Newman and Reza, 1979). Thus, the relatively focal grey matter density findings may reflect the anatomy of cerebello-cerebral networks.

While the negative association between grey matter density and cognitive function in the patient group must be interpreted with caution given the moderate sample size, we note that this association was strongest for the cognitive domains of processing speed and executive function (where all tests included in the latter category also relied on speeded responses). Supporting this structure-cognition association, the cingulate cortex is a consistent

Table 5
Relationships between clinical variables and structural MRI-indices.

	F-value	*t*-Value[a]	Effect size[a,b]	*p*-Value[a]
Grey matter density[c]				
Age	2.182	1.477	.127	.160
Sex	1.247	1.117	.077	.282
Lesion size	.11	−.335	.007	.742
Ventricle volume	8.790	2.965	.369	**.010**
Fractional anisotropy[c]				
Age	.215	−.464	.014	.649
Sex	7.153	−2.675	.323	**.017**
Lesion size	3.052	−1.747	.169	.101
Ventricle volume	3.498	−1.870	.189	.081
Mean diffusivity[c]				
Age	< .001	.010	< .001	.992
Sex	.998	.999	.062	.334
Lesion size	2.403	1.550	.138	.142
Ventricle volume	7.293	2.701	.327	**.016**
Axial diffusivity[c]				
Age	.333	−.577	.022	.573
Sex	.031	.177	.002	.862
Lesion size	.005	−.072	< .001	.943
Ventricle volume	13.294	3.646	.470	**.002**
Radial diffusivity[c]				
Age	.033	.182	.002	.858
Sex	4.042	2.010	.212	.063
Lesion size	6.871	2.621	.314	**.019**
Ventricle volume	9.067	3.011	.377	**.009**

[a] *t*-Values, *p*-Values and effect sizes are based on GLMs with sex as a fixed factors and age, lesion size and ventricle size as covariates.
[b] Partial eta squared. *ps* < .05 are marked in bold.
[c] Averaged across all voxels showing significant group difference.

finding across a series of neuroimaging studies investigating functional and structural associations with response speed (Grinband et al., 2011; Grinband et al., 2008; Hahn et al., 2007; Yarkoni et al., 2009), as well as various aspects of executive functions (Niendam et al., 2012; Westlye et al., 2011). We further observe that the grey matter density clusters partially overlap the default mode network (medial prefrontal cortex, posterior cingulate and the hippocampus). While no other structure-function associations emerged as significant, changes in the default mode network could potentially be related to the patients' reduced performance on tests of episodic memory (Sestieri et al., 2011). Other brain networks overlapping the GMD clusters include the salience network (i.e., the anterior cingulate region discussed above) and, to a lesser degree, a sensori-motor network (supplementary motor area).

On a methodological note, our finding of significant group differences in the analysis of grey matter density (unmodulated maps) but not grey matter volume (modulated maps), are in line with a recent study reporting that modulation resulted in significantly reduced sensitivity to detect abnormalities in simulated datasets where the "ground truth" is known (Radua et al., 2014). Importantly, the increased sensitivity for analyses without a modulation step did not come at the cost of an increased false positive rate (Radua et al., 2014).

4.2. Possible mechanisms

In the current study, we examined two potential mechanisms accounting for group differences in cognitive function and brain structure: 1) effects of cerebellar tissue loss through remote neurodegeneration (Viscomi and Molinari, 2014) and/or altered brain development (Limperopoulos et al., 2012; Wang et al., 2014) and 2) effects of concomitant hydrocephalus (Hattori et al., 2012; Scheel et al., 2012; Yuan et al., 2013). While we did not have data on the degree of pre-surgical hydrocephalus in the current group of patients (likely present to some extent in all), we calculated current lateral ventricle volume as a putative marker of previous hydrocephalus severity. As expected, ventricular volumes were increased in patients relative to controls. Moreover, within the patient group, larger ventricular volume was significantly associated with increased grey matter density and altered white matter microstructure, with the largest effect seen for AD, consistent with recent findings in hydrocephalus patients (Cauley and Cataltepe, 2014). Importantly, however, all reported group differences remained significant when ventricular volume was included as a covariate in the analyses, and we also observed an association between cerebellar lesion size and RD. These results suggest that the observed group differences in supratentorial brain structure may only partly be attributed to hydrocephalus.

4.3. Limitations

The main limitation of the current study was the moderate sample size, and especially the analyses of possible mechanisms and structure-function associations need to be interpreted with this limitation in mind. In particular, larger patient samples would be needed to map the specificity of cerebral effects associated with lesions to different cerebellar regions. Second, while previous studies support the use of current ventricle volume as an indirect measure of previous hydrocephalus severity (Santamarta et al., 2008; St George et al., 2004), the degree to which current and previous ventricle volumes correspond is unknown. Future studies with detailed information on the presence, duration, and severity of hydrocephalus are needed.

A third potential limitation concerns the matching of the control group to the cerebellar patients as both years of completed education and estimated IQ were significantly reduced in patients relative to controls. Six of the patients also fulfilled the ICD-10 diagnostic criteria for current (four patients) or previous (two patients) psychiatric disorder. IQ is usually not affected following cerebellar pathology in adults (Alexander et al., 2012; Timmann and Daum, 2010), but moderate reductions have been observed following lesions acquired in childhood (Beebe, 2005; Rønning

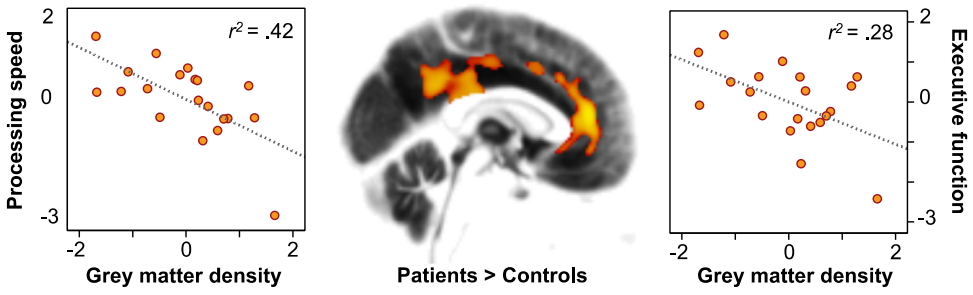

Fig. 4. Scatter-plots showing the correlations between mean grey matter density (across the cerebral cluster showing a significant group difference) and performance on neuropsychological tests of processing speed (left) and executive function (right). The plots show standardized scores corrected for effects of sex and age.

et al., 2005), suggesting an interaction between cerebellar insult and developmental stage (Timmann and Daum, 2010). Further, the magnitude of the IQ-reduction in the current study corresponds to previous findings in a large sample ($N=91$) of cerebellar astrocytoma patients (Beebe, 2005). Thus, we believe the observed IQ differences primarily reflect long-term effects of the early lesions. Importantly, all group differences in brain structure, and most performance differences on neuropsychological tests, remained significant when including IQ as a covariate in the analyses. Likewise, restricting the analyses to patients with no lifetime history of psychiatric disorder only minimally affected the results.

Fourth, we were unable to reliably link the observed white matter changes to cognitive function. Of note, previous reports of such associations come from studies of patients with cerebellar medulloblastomas (Brinkman et al., 2012; Khong et al., 2003; Mabbott et al., 2006; Mulhern et al., 2001; Reddick et al., 2003), where treatment includes radiation and chemotherapy and cognitive deficits tend to be more pronounced (Rønning et al., 2005). Possibly, a larger sample would be required to reveal such associations in the less affected patients with cerebellar astrocytomas.

Finally, the relationships between the MRI-based indices used in the current study and the underlying cellular microstructure are as yet incompletely understood. Several anatomical features may account for differences in grey matter density, including cortical thickness, cortical area, local folding patterns (Mechelli et al., 2005) and degree of cortical myelination (Taki et al., 2013). Similarly, whereas caution is warranted (Wheeler-Kingshott, 2009), differences in the DTI-indices may be related to variability in axon integrity and myelination (Beaulieu, 2009), the relative amount of parallel and crossing fibres within voxels (Walhovd et al., 2014) and/or axonal packing density (Cauley and Cataltepe, 2014). It is also an open question whether the group differences not attributable to hydrocephalus primarily reflect remote neurodegeneration (Viscomi and Molinari, 2014), disrupted brain development (Wang et al., 2014) or compensatory reorganisation (Dancause et al., 2005; Eisner-Janowicz et al., 2008; Gauthier et al., 2008; Sterling et al., 2013). Longitudinal studies of brain development and plasticity related to functional recovery following cerebellar lesions in both animal models and cerebellar patients are needed to investigate such mechanisms in further detail.

4.4. Conclusions

In conclusion, we observed reduced cognitive function, focally increased grey matter density and widespread white matter microstructural abnormalities in patients with focal cerebellar lesions following tumour surgery in their childhood. Whereas group differences could not be entirely accounted for by increased ventricle volumes in patients, concomitant hydrocephalus is likely a partial explanation for some of the effects, and the potential impact of hydrocephalus needs to be considered when interpreting previous and future findings in this patient group. Finally, our finding of increased grey matter density in patients with cerebellar tumour resections in childhood and adolescence stand in marked contrast to results from previous studies of patients with both perinatal and adult cerebellar injury. Seen together, these studies suggest that the developmental stage at the time of cerebellar injury may modulate effects on supratentorial brain structure and/or that the structural manifestations of altered developmental trajectories may depend on the age at testing.

Funding

This research was supported by a grant from the South Norway Health Authority (3b-122). L.T.W. was funded by The Research Council of Norway (204966/F20).

Acknowledgements

We thank the participants in this study for their time and effort, Dr. Robert T. Knight for quality control of reconstructed lesions, and the reviewers for helpful comments on an earlier version of the manuscript.

Appendix A. Supplementary information

Supplementary data associated with this article can be found in the online version at http://dx.doi.org/10.1016/j.neuropsychologia.2015.02.007.

References

Aarsen, F.K., Arts, W.F.M., Van Veelen-Vincent, M.L.C., Lequin, M.H., Catsman-Berrevoets, C.E., 2014. Long-term outcome in children with low grade tectal tumours and obstructive hydrocephalus. Eur. J. Paediatr. Neurol.: Off. J. Eur. Paediatr. Neurol. Soc. 18 (4), 469–474. http://dx.doi.org/10.1016/j.ejpn.2014.03.002.

Aarsen, F.K., Van Dongen, H.R., Paquier, P.F., Van Mourik, M., Catsman-Berrevoets, C.E., 2004. Long-term sequelae in children after cerebellar astrocytoma surgery. Neurology 62 (8), 1311–1316. http://dx.doi.org/10.1212/01.WNL.0000120549.77188.36.

Alexander, M.P., Gillingham, S., Schweizer, T., Stuss, D.T., 2012. Cognitive impairments due to focal cerebellar injuries in adults. Cortex 48 (8), 980–990. http://dx.doi.org/10.1016/j.cortex.2011.03.012.

Ashburner, J., 2007. A fast diffeomorphic image registration algorithm. Neuroimage 38 (1), 95–113. http://dx.doi.org/10.1016/j.neuroimage.2007.07.007.

Ayling, E., Aghajani, M., Fouche, J.-P., van der Wee, N., 2012. Diffusion tensor imaging in anxiety disorders. Curr. Psychiatry Rep. *14* (3), 197–202. http://dx.doi.org/10.1007/s11920-012-0273-z.

Balsters, J.H., Laird, A.R., Fox, P.T., Eickhoff, S.B., 2014. Bridging the gap between functional and anatomical features of cortico-cerebellar circuits using meta-analytic connectivity modeling. Hum. Brain Mapp. *35* (7), 3152–3169. http://dx.doi.org/10.1002/hbm.22392.

Basser, P.J., Pierpaoli, C., 1996. Microstructural and physiological features of tissues elucidated by quantitative-diffusion-tensor MRI. J. Magn. Reson. Ser. B 111 (3), 209–219 (Retrieved from)⟨http://eutils.ncbi.nlm.nih.gov/entrez/eutils/elink.fcgi?dbfrom=pubmed&id=8661285&retmode=ref&cmd=prlinks⟩.

Beaulieu, C., 2009. The biological basis of diffusion ansisotropy In: Johansen-Berg, H., Behrens, T.E.J. (Eds.), Diffusion MRI: From quantitative measurement to in-vivo neuroanatomy, 1st ed. Academic Press, Amsterdam, Boston, Heidelberg, London, New York, Oxford, Paris, San Diego, Singapore, Sydney, Tokyo, pp. 105–126.

Beebe, D.W., 2005. Cognitive and adaptive outcome in low-grade pediatric cerebellar astrocytomas: evidence of diminished cognitive and adaptive functioning in national collaborative research studies (CCG 9891/POG 9130). J. Clin. Oncol.: Off. J. Am. Soc. Clin. Oncol. *23* (22), 5198–5204. http://dx.doi.org/10.1200/JCO.2005.06.117.

Benedict, R.H.B., 1997. Brief Visuospatial Memory Test–revised. Psychological Assessment Resources, Inc., Odessa.

Bernard, J.A., Peltier, S.J., Benson, B.L., Wiggins, J.L., Jaeggi, S.M., Buschkuehl, M., et al., 2014. Dissociable functional networks of the human dentate nucleus. Cereb. Cortex *24* (8), 2151–2159. http://dx.doi.org/10.1093/cercor/bht065.

Bernard, J.A., Seidler, R.D., Hassevoort, K.M., Benson, B.L., Welsh, R.C., Wiggins, J.L., et al., 2012. Resting state cortico-cerebellar functional connectivity networks: a comparison of anatomical and self-organizing map approaches. Front. Neuroanat. *6*, 31. http://dx.doi.org/10.3389/fnana.2012.00031.

Bolduc, M.-E., Plessis, du, A.J., Evans, A., Guizard, N., Zhang, X., Robertson, R.L., Limperopoulos, C., 2011. Cerebellar malformations alter regional cerebral development. Dev. Med. Child Neurol. *53* (12), 1128–1134. http://dx.doi.org/10.1111/j.1469-8749.2011.04090.x.

Bora, E., Fornito, A., Pantelis, C., Yücel, M., 2012. Gray matter abnormalities in Major Depressive Disorder: a meta-analysis of voxel based morphometry studies. J. Affect. Disord. *138* (1-2), 9–18. http://dx.doi.org/10.1016/j.jad.2011.03.049.

Bostan, A.C., Dum, R.P., Strick, P.L., 2013. Cerebellar networks with the cerebral cortex and basal ganglia. Trends Cogn. Sci. *17* (5), 241–254. http://dx.doi.org/10.1016/j.tics.2013.03.003.

Brinkman, T.M., Reddick, W.E., Luxton, J., Glass, J.O., Sabin, N.D., Srivastava, D.K., et al., 2012. Cerebral white matter integrity and executive function in adult survivors of childhood medulloblastoma. Neuro-Oncol. 14 (suppl 4), iv25–iv36. http://dx.doi.org/10.1093/neuonc/nos214.

Brown, T.T., Kuperman, J.M., Chung, Y., Erhart, M., McCabe, C., Hagler, D.J., et al., 2012. Neuroanatomical assessment of biological maturity. Curr. Biol. *22* (18), 1693–1698. http://dx.doi.org/10.1016/j.cub.2012.07.002.

Buckner, R.L., Krienen, F.M., Castellanos, A., Diaz, J.C., Yeo, B.T.T., 2011. The organization of the human cerebellum estimated by intrinsic functional connectivity. J. Neurophysiol. *106* (5), 2322–2345. http://dx.doi.org/10.1152/jn.00339.2011.

Castaneda, A.E., Tuulio-Henriksson, A., Marttunen, M., Suvisaari, J., Lönnqvist, J., 2008. A review on cognitive impairments in depressive and anxiety disorders with a focus on young adults. J. Affect. Disord. *106* (1-2), 1–27. http://dx.doi.org/10.1016/j.jad.2007.06.006.

Cauley, K.A., Cataltepe, O., 2014. Axial diffusivity of the corona radiata correlated with ventricular size in adult hydrocephalus. Am. J. Roentgenol. *203* (1), 170–179. http://dx.doi.org/10.2214/AJR.12.10009.

Clausi, S., Bozzali, M., Leggio, M.G., Di Paola, M., Hagberg, G.E., Caltagirone, C., Molinari, M., 2009. Quantification of gray matter changes in the cerebral cortex after isolated cerebellar damage: a voxel-based morphometry study. Neuroscience *162* (3), 827–835. http://dx.doi.org/10.1016/j.neuroscience.2009.02.001.

Cohen, J., 1992. A power primer. Psychol. Bull. 112 (1), 155–159.

Dancause, N., Barbay, S., Frost, S.B., Plautz, E.J., Chen, D., Zoubina, E.V., et al., 2005. Extensive cortical rewiring after brain injury. J. Neurosci. *25* (44), 10167–10179. http://dx.doi.org/10.1523/JNEUROSCI.3256-05.2005.

Daniels, J.K., Lamke, J.-P., Gaebler, M., Walter, H., Scheel, M., 2013. White matter integrity and its relationship to PTSD and childhood trauma–a systematic review and meta-analysis. Depress. Anxiety *30* (3), 207–216. http://dx.doi.org/10.1002/da.22044.

Delis, D.C., Kaplan, E., Kramer, J.H., 2001. Delis–Kaplan Executive Function System. San Antonio: the Psychological Corporation.

Delis, D.C., Kramer, J.H., Kaplan, E., Ober, B.A., 2000. California Verbal Learning Test – Second Edition (CVLT-II) Manual. San Antonio: the Psychological Corporation.

Diedrichsen, J., 2006. A spatially unbiased atlas template of the human cerebellum. Neuroimage *33* (1), 127–138. http://dx.doi.org/10.1016/j.neuroimage.2006.05.065.

Due-Tønnessen, B.J., Lundar, T., Egge, A., Scheie, D., 2013. Neurosurgical treatment of low-grade cerebellar astrocytoma in children and adolescents: a single consecutive institutional series of 100 patients. J. Neurosurg. *11* (3), 245–249. http://dx.doi.org/10.3171/2012.11.PEDS12265 (*Pediatrics*,).

E, K.-H., Chen, S.-H.A., Ho, M.-H.R., Desmond, J.E., 2014. A meta-analysis of cerebellar contributions to higher cognition from PET and fMRI studies. Hum. Brain Mapp. *35* (2), 593–615. http://dx.doi.org/10.1002/hbm.22194.

Eckert, M.A., Tenforde, A., Galaburda, A.M., Bellugi, U., Korenberg, J.R., Mills, D., Reiss, A.L., 2006. To modulate or not to modulate: differing results in uniquely shaped Williams syndrome brains. Neuroimage *32* (3), 1001–1007. http://dx.doi.org/10.1016/j.neuroimage.2006.05.014.

Eisner-Janowicz, I., Barbay, S., Hoover, E., Stowe, A.M., Frost, S.B., Plautz, E.J., Nudo, R.J., 2008. Early and late changes in the distal forelimb representation of the supplementary motor area after injury to frontal motor areas in the squirrel monkey. J. Neurophysiol. *100* (3), 1498–1512. http://dx.doi.org/10.1152/jn.90447.2008.

Fjell, A.M., Westlye, L.T., Amlien, I., Tamnes, C.K., Grydeland, H., Engvig, A., et al., 2015. High-expanding cortical regions in human development and evolution are related to higher intellectual abilities. Cereb. Cortex *1*, 26–34. http://dx.doi.org/10.1093/cercor/bht201.

Galgiani, J.E., 2013. Vermis-cingulate cortex interconnections: a cerebro-cerebellar circuit in the rat. University of Pittsburgh, Pittsburgh (Master's thesis).

Gauthier, L.V., Taub, E., Perkins, C., Ortmann, M., Mark, V.W., Uswatte, G., 2008. Remodeling the brain: plastic structural brain changes produced by different motor therapies after stroke. Stroke: J. Cereb. Circ. *39* (5), 1520–1525. http://dx.doi.org/10.1161/STROKEAHA.107.502229.

Grinband, J., Savitskaya, J., Wager, T.D., Teichert, T., Ferrera, V.P., Hirsch, J., 2011. The dorsal medial frontal cortex is sensitive to time on task, not response conflict or error likelihood. Neuroimage *57* (2), 303–311. http://dx.doi.org/10.1016/j.neuroimage.2010.12.027.

Grinband, J., Wager, T.D., Lindquist, M., Ferrera, V.P., Hirsch, J., 2008. Detection of time-varying signals in event-related fMRI designs. Neuroimage *43* (3), 509–520. http://dx.doi.org/10.1016/j.neuroimage.2008.07.065.

Gudrunardottir, T., Sehested, A., Juhler, M., Schmiegelow, K., 2011. Cerebellar mutism: review of the literature. Child's Nerv. Syst.: Off. J. Int. Soc. Pediatr. Neurosurg. *27* (3), 355–363. http://dx.doi.org/10.1007/s00381-010-1328-2.

Habas, C., Kamdar, N., Nguyen, D., Prater, K., Beckmann, C.F., Menon, V., Greicius, M. D., 2009. Distinct cerebellar contributions to intrinsic connectivity networks. J. Neurosci. *29* (26), 8586–8594. http://dx.doi.org/10.1523/JNEUROSCI.1868-09.2009.

Habas, C., Shirer, W.R., Greicius, M.D., 2013. Delineation of cerebrocerebellar networks with MRI measures of functional and structural connectivity In: Manto, M., Gruol, J.D., Schmahmann, J.D., Koibuchi, F., Rossi, F. (Eds.), Handbook of the Cerebellum and Cerebellar Disorders. Springer, Dordrecht, The Netherlands, pp. 571–585. http://dx.doi.org/10.1007/978-94-007-1333-8_26.

Hahn, B., Ross, T.J., Stein, E.A., 2007. Cingulate activation increases dynamically with response speed under stimulus unpredictability. Cereb. Cortex 17 (7), 1664–1671. http://dx.doi.org/10.1093/cercor/bhl075.

Hattori, T., Ito, K., Aoki, S., Yuasa, T., Sato, R., Ishikawa, M., et al., 2012. White matter alteration in idiopathic normal pressure hydrocephalus: tract-based spatial statistics study. Am. J. Neuroradiol. *33* (1), 97–103. http://dx.doi.org/10.3174/ajnr.A2706.

Heath, R.G., Harper, J.W., 1974. Ascending projections of the cerebellar fastigial nucleus to the hippocampus, amygdala, and other temporal lobe sites: evoked potential and histological studies in monkeys and cats. Exp. Neurol. *45* (2), 268–287.

Heath, R.G., Dempesy, C.W., Fontana, C.J., Myers, W.A., 1978. Cerebellar stimulation: effects on septal region, hippocampus, and amygdala of cats and rats. Biol. Psychiatry *13* (5), 501–529.

Henley, S.M.D., Ridgway, G.R., Scahill, R.I., Klöppel, S., Tabrizi, S.J., Fox, N.C., et al., 2010. Pitfalls in the use of voxel-based morphometry as a biomarker: examples from huntington disease. Am. J. Neuroradiol. *31* (4), 711–719. http://dx.doi.org/10.3174/ajnr.A1939.

Hensch, T.K., 2005. Critical period plasticity in local cortical circuits. Nat. Rev. Neurosci. *6* (11), 877–888. http://dx.doi.org/10.1038/nrn178.

Hoang, D.H., Pagnier, A., Guichardet, K., Dubois-Teklali, F., Schiff, I., Lyard, G., et al., 2014. Cognitive disorders in pediatric medulloblastoma: what neuroimaging has to offer. J. Neurosurg. Pediatr., 1–9. http://dx.doi.org/10.3171/2014.5.PEDS13571.

Jenkinson, M., Bannister, P., Brady, M., Smith, S., 2002. Improved optimization for the robust and accurate linear registration and motion correction of brain images. Neuroimage 17 (2), 825–841 (Retrieved from)⟨http://eutils.ncbi.nlm.nih.gov/entrez/eutils/elink.fcgi?dbfrom=pubmed&id=12377157&retmode=ref&cmd=prlinks⟩.

Jissendi, P., Baudry, S., Balériaux, D., 2008. Diffusion tensor imaging (DTI) and tractography of the cerebellar projections to prefrontal and posterior parietal cortices: a study at 3T. J. Neuroradiol. *35* (1), 42–50. http://dx.doi.org/10.1016/j.neurad.2007.11.001.

Kameda-Smith, M.M., White St, M.A.J., George, E.J., Brown, J.I.M., 2013. Time to diagnosis of paediatric posterior fossa tumours: an 11-year West of Scotland experience 2000–2011. Br. J. Neurosurg. *27* (3), 364–369. http://dx.doi.org/10.3109/02688697.2012.741731.

Kelly, R.M., Strick, P.L., 2003. Cerebellar loops with motor cortex and prefrontal cortex of a nonhuman primate. J. Neurosci. *23* (23), 8432–8444.

Kempton, M.J., Underwood, T.S.A., Brunton, S., Stylios, F., Schmechtig, A., Ettinger, U., et al., 2011. A comprehensive testing protocol for MRI neuroanatomical segmentation techniques: evaluation of a novel lateral ventricle segmentation method. Neuroimage *58* (4), 1051–1059. http://dx.doi.org/10.1016/j.neuroimage.2011.06.080.

Khong, P.-L., Kwong, D.L.W., Chan, G.C.F., Sham, J.S.T., Chan, F.-L., Ooi, G.-C., 2003. Diffusion-tensor imaging for the detection and quantification of treatment-induced white matter injury in children with medulloblastoma: a pilot study. Am. J. Neuroradiol. 24 (4), 734–740 (Retrieved from)⟨http://eutils.ncbi.nlm.nih.gov/entrez/eutils/elink.fcgi?dbfrom=pubmed&id=12695214&retmode=ref&cmd=prlinks⟩.

Krienen, F.M., Buckner, R.L., 2009. Segregated fronto-cerebellar circuits revealed by intrinsic functional connectivity. *Cereb. Cortex, 19*(10), 2009, 2485–2497. http://dx.doi.org/10.1093/cercor/bhp135.

Leung, L.H.T., Ooi, G.-C., Kwong, D.L.W., Chan, G.C.F., Cao, G., Khong, P.-L., 2004. White-matter diffusion anisotropy after chemo-irradiation: a statistical parametric mapping study and histogram analysis. Neuroimage *21* (1), 261–268.

Liao, Y., Huang, X., Wu, Q., Yang, C., Kuang, W., Du, M., et al., 2013. Is depression a disconnection syndrome? Meta-analysis of diffusion tensor imaging studies in patients with MDD. J. Psychiatry Neurosci. *38* (1), 49–56. http://dx.doi.org/10.1503/jpn.110180.

Limperopoulos, C., Chilingaryan, G., Guizard, N., Robertson, R.L., Plessis, du, A.J., 2010. Cerebellar injury in the premature infant is associated with impaired growth of specific cerebral regions. Pediatr. Res. *68* (2), 145–150. http://dx.doi.org/10.1203/PDR.0b013e3181e1d032.

Limperopoulos, C., Chilingaryan, G., Sullivan, N., Guizard, N., Robertson, R.L., Plessis, du, A.J., 2014. Injury to the premature cerebellum: outcome is related to remote cortical development. Cereb. Cortex *24* (3), 728–736. http://dx.doi.org/10.1093/cercor/bhs354.

Limperopoulos, C., Soul, J.S., Haidar, H., Huppi, P.S., Bassan, H., Warfield, S.K., et al., 2005. Impaired trophic interactions between the cerebellum and the cerebrum among preterm infants. Pediatrics *116* (4), 844–850. http://dx.doi.org/10.1542/peds.2004-2282.

Lyall A.E., Shi F., Geng X., Woolson S., Li G., Wang L., et al., Dynamic development of regional cortical thickness and surface area in early childhood Cereb. Cortex (in press), http://dx.doi.org/10.1093/cercor/bhu027.

Mabbott, D.J., Noseworthy, M.D., Bouffet, E., Rockel, C., Laughlin, S., 2006. Diffusion tensor imaging of white matter after cranial radiation in children for medulloblastoma: correlation with IQ. Neuro-Oncol. *8* (3), 244–252. http://dx.doi.org/10.1215/15228517-2006-002.

Mariën, P., De Smet, H.J., Paquier, P.F., Verhoeven, J., 2010. Cerebellocerebral diaschisis and postsurgical posterior fossa syndrome in pediatric patients. Am. J. Neuroradiol. 31 (9). http://dx.doi.org/10.3174/ajnr.A2198 (E82–author reply E83).

Mechelli, A., Price, C., Friston, K., Ashburner, J., 2005. Voxel-based morphometry of the human brain: methods and applications. Curr. Med. Imaging Rev. *150* (2), 105–113. http://dx.doi.org/10.1007/s00701-007-1477-6.

Middleton, F.A., Strick, P.L., 1994. Anatomical evidence for cerebellar and basal ganglia involvement in higher cognitive function. Science *266* (5184), 458–461.

Miller, N.G., Reddick, W.E., Kocak, M., Glass, J.O., Löbel, U., Morris, B., et al., 2010. Cerebellocerebral diaschisis is the likely mechanism of postsurgical posterior fossa syndrome in pediatric patients with midline cerebellar tumors. Am. J. Neuroradiol. *31* (2), 288–294. http://dx.doi.org/10.3174/ajnr.A1821.

Mulhern, R.K., Palmer, S.L., Reddick, W.E., Glass, J.O., Kun, L.E., Taylor, J., et al., 2001. Risks of young age for selected neurocognitive deficits in medulloblastoma are associated with white matter loss. J. Clin. Oncol.: Off. J. Am. Soc. Clin. Oncol. 19 (2), 472–479 (Retrieved from)⟨http://eutils.ncbi.nlm.nih.gov/entrez/eutils/elink.fcgi?dbfrom=pubmed&id=11208841&retmode=ref&cmd=prlinks⟩.

Newman, P.P., Reza, H., 1979. Functional relationships between the hippocampus and the cerebellum: an electrophysiological study of the cat. J. Physiol. *287*, 405–426.

Niendam, T.A., Laird, A.R., Ray, K.L., Dean, Y.M., Glahn, D.C., Carter, C.S., 2012. Meta-analytic evidence for a superordinate cognitive control network subserving diverse executive functions. Cogn. Affect. Behav. Neurosci. *12* (2), 241–268. http://dx.doi.org/10.3758/s13415-011-0083-5.

O'Reilly, J.X., Beckmann, C.F., Tomassini, V., Ramnani, N., Johansen-Berg, H., 2010. Distinct and overlapping functional zones in the cerebellum defined by resting state functional connectivity. Cereb. Cortex *20* (4), 953–965. http://dx.doi.org/10.1093/cercor/bhp157.

Omar, D., Ryan, T., Carson, A., Bak, T.H., Torrens, L., Whittle, I., 2014. Clinical and methodological confounders in assessing the cerebellar cognitive affective syndrome in adult patients with posterior fossa tumours. Br. J. Neurosurg., 1–10. http://dx.doi.org/10.3109/02688697.2014.920487.

Palesi, F., Tournier, J.-D., Calamante, F., Muhlert, N., Castellazzi, G., Chard, D., et al., 2014. Contralateral cerebello-thalamo-cortical pathways with prominent involvement of associative areas in humans in vivo. Brain Struct. Funct. . http://dx.doi.org/10.1007/s00429-014-0861-2

Radua, J., Canales-Rodríguez, E.J., Pomarol-Clotet, E., Salvador, R., 2014. Validity of modulation and optimal settings for advanced voxel-based morphometry. Neuroimage *86*, 81–90. http://dx.doi.org/10.1016/j.neuroimage.2013.07.084.

Ramnani, N., 2006. The primate cortico-cerebellar system: anatomy and function. Nat. Rev. Neurosci. *7* (7), 511–522. http://dx.doi.org/10.1038/nrn1953.

Reddick, W.E., White, H.A., Glass, J.O., Wheeler, G.C., Thompson, S.J., Gajjar, A., et al., 2003. Developmental model relating white matter volume to neurocognitive deficits in pediatric brain tumor survivors. Cancer *97* (10), 2512–2519. http://dx.doi.org/10.1002/cncr.11355.

Ridgway, G., Barnes, J., Pepple, T., Fox, N., 2011. Estimation of intracranial volume: a comparison of methods. Alzheimer's Dement., 7 (4), s62–s63. http://dx.doi.org/10.1016/j.jalz.2011.05.099.

Rock, P.L., Roiser, J.P., Riedel, W.J., Blackwell, A.D., 2013. Cognitive impairment in depression: a systematic review and meta-analysis. Psychol. Med., 1–12. http://dx.doi.org/10.1017/S0033291713002535.

Rorden, C., Karnath, H.-O., Bonilha, L., 2007. Improving lesion-symptom mapping. J. Cogn. Neurosci. *19* (7), 1081–1088. http://dx.doi.org/10.1162/jocn.2007.19.7.1081.

Rueckriegel, S.M., Driever, P.H., Blankenburg, F., Lüdemann, L., Henze, G., Bruhn, H., 2010. Differences in supratentorial damage of white matter in pediatric survivors of posterior fossa tumors with and without adjuvant treatment as detected by magnetic resonance diffusion tensor imaging. Int. J. Radiat. Oncol. Biol. Phys. *76* (3), 859–866. http://dx.doi.org/10.1016/j.ijrobp.2009.02.054.

Rønning, C., Sundet, K., Due-Tønnessen, B., Lundar, T., Helseth, E., 2005. Persistent cognitive dysfunction secondary to cerebellar injury in patients treated for posterior fossa tumors in childhood. Pediatr. Neurosurg. *41* (1), 15–21. http://dx.doi.org/10.1159/000084860.

Sang, L., Qin, W., Liu, Y., Han, W., Zhang, Y., Jiang, T., Yu, C., 2012. Resting-state functional connectivity of the vermal and hemispheric subregions of the cerebellum with both the cerebral cortical networks and subcortical structures. Neuroimage *61* (4), 1213–1225. http://dx.doi.org/10.1016/j.neuroimage.2012.04.011.

Santamarta, D., Martin-Vallejo, J., Díaz-Alvarez, A., Maillo, A., 2008. Changes in ventricular size after endoscopic third ventriculostomy. Acta Neurochir. 150 (2). http://dx.doi.org/10.1007/s00701-007-1477-6 (119–27– discussion 127).

Scheel, M., Diekhoff, T., Sprung, C., Hoffmann, K.-T., 2012. Diffusion tensor imaging in hydrocephalus–findings before and after shunt surgery. Acta Neurochir. *154* (9), 1699–1706. http://dx.doi.org/10.1007/s00701-012-1377-2.

Schmitz-Hübsch, T., Montcel, du, S.T., Baliko, L., Berciano, J., Boesch, S., Depond, C., et al., 2006. Scale for the assessment and rating of ataxia: development of a new clinical scale. Neurology *66* (11), 1717–1720. http://dx.doi.org/10.1212/01.wnl.0000219042.60538.92.

Schnack, H.G., van Haren, N.E.M., Brouwer, R.M., Evans, A., Durston, S., Boomsma, D. I., et al., Changes in thickness and surface area of the human cortex and their relationship with intelligence. Cereb. Cortex (in press), http://dx.doi.org/10.1093/cercor/bht357.

Scott, R.B., Stoodley, C.J., Anslow, P., Paul, C., Stein, J.F., Sugden, E.M., Mitchell, C.D., 2001. Lateralized cognitive deficits in children following cerebellar lesions. Dev. Med. Child Neurol. *43* (10), 685–691.

Seghier, M.L., Ramlackhansingh, A., Crinion, J., Leff, A.P., Price, C.J., 2008. Lesion identification using unified segmentation-normalisation models and fuzzy clustering. Neuroimage *41* (4), 1253–1266. http://dx.doi.org/10.1016/j.neuroimage.2008.03.028.

Sestieri, C., Corbetta, M., Romani, G.L., Shulman, G.L., 2011. Episodic memory retrieval, parietal cortex, and the default mode network: functional and topographic analyses. J. Neurosci. *31* (12), 4407–4420. http://dx.doi.org/10.1523/JNEUROSCI.3335-10.2011.

Shang, J., Fu, Y., Ren, Z., Zhang, T., Du, M., Gong, Q., et al., 2014. The common traits of the ACC and PFC in anxiety disorders in the DSM-5: meta-analysis of voxel-based morphometry studies. PloS One *9* (3), e93432. http://dx.doi.org/10.1371/journal.pone.0093432.

Shaw, P., Kabani, N.J., Lerch, J.P., Eckstrand, K., Lenroot, R., Gogtay, N., et al., 2008. Neurodevelopmental trajectories of the human cerebral cortex. J. Neurosci. *28* (14), 3586–3594. http://dx.doi.org/10.1523/JNEUROSCI.5309-07.2008.

Sheehan, D.V., Lecrubier, Y., Sheehan, K.H., Amorim, P., Janavs, J., Weiller, E., et al., 1998. The Mini-International Neuropsychiatric Interview (M.I.N.I.): the development and validation of a structured diagnostic psychiatric interview for DSM-IV and ICD-10. J. Clin. Psychiatry *59* (Suppl 20), s22-s33, quiz 34-57. http://www.ncbi.nlm.nih.gov/pubmed/9881538.

Simó, M., Rifà-Ros, X., Rodriguez-Fornells, A., Bruna, J., 2013. Chemobrain: a systematic review of structural and functional neuroimaging studies. Neurosci. Biobehav. Rev. 37 (8), 1311–1321. http://dx.doi.org/10.1016/j.neubiorev.2013.04.015.

Smith, S.M., 2002. Fast robust automated brain extraction. Hum. Brain Mapp. *17* (3), 143–155. http://dx.doi.org/10.1002/hbm.10062.

Smith, S.M., Nichols, T.E., 2009. Threshold-free cluster enhancement: addressing problems of smoothing, threshold dependence and localisation in cluster inference. Neuroimage *44* (1), 83–98. http://dx.doi.org/10.1016/j.neuroimage.2008.03.061.

Smith, S.M., Jenkinson, M., Johansen-Berg, H., Rueckert, D., Nichols, T.E., Mackay, C. E., et al., 2006. Tract-based spatial statistics: voxelwise analysis of multi-subject diffusion data. Neuroimage *31* (4), 1487–1505. http://dx.doi.org/10.1016/j.neuroimage.2006.02.024.

Smith, S.M., Jenkinson, M., Woolrich, M.W., Beckmann, C.F., Behrens, T.E.J., Johansen-Berg, H., et al., 2004. Advances in functional and structural MR image analysis and implementation as FSL. Neuroimage *23* (Suppl 1,), S208. http://dx.doi.org/10.1016/j.neuroimage.2004.07.051 (19).

Soelva, V., Hernáiz Driever, P., Abbushi, A., Rueckriegel, S., Bruhn, H., Eisner, W., Thomale, U.-W., 2013. Fronto-cerebellar fiber tractography in pediatric patients following posterior fossa tumor surgery. Child's Nerv. Syst.: Off. J. Int. Soc. Pediatr. Neurosurg. *29* (4), 597–607. http://dx.doi.org/10.1007/s00381-012-1973-8.

St George, E., Natarajan, K., Sgouros, S., 2004. Changes in ventricular volume in hydrocephalic children following successful endoscopic third ventriculostomy. Child's Nerv. Syst.: Off. J. Int. Soc. Pediatr. Neurosurg. *20* (11–12), 834–838. http://dx.doi.org/10.1007/s00381-004-0939-x.

Steinlin, M., 2007. The cerebellum in cognitive processes: supporting studies in children. The Cerebellum *6* (3), 237–241. http://dx.doi.org/10.1080/14734220701344507.

Steinlin, M., Imfeld, S., Zulauf, P., Boltshauser, E., Lövblad, K.-O., Ridolfi Lüthy, A., et al., 2003. Neuropsychological long-term sequelae after posterior fossa tumour resection during childhood. Brain :J. Neurol. 126 (Pt 9), 1998–2008. http://dx.doi.org/10.1093/brain/awg195.

Sterling, C., Taub, E., Davis, D., Rickards, T., Gauthier, L.V., Griffin, A., Uswatte, G., 2013. Structural neuroplastic change after constraint-induced movement therapy in children with cerebral palsy. Pediatrics *131* (5), e1664. http://dx.doi.org/10.1542/peds.2012-2051 (9).

Stoodley, C.J., Schmahmann, J.D., 2009. Functional topography in the human cerebellum: a meta-analysis of neuroimaging studies. Neuroimage *44* (2), 489–501. http://dx.doi.org/10.1016/j.neuroimage.2008.08.039.

Strick, P.L., Dum, R.P., Fiez, J.A., 2009. Cerebellum and nonmotor function. Annu. Rev. Neurosci. *32* (1), 413–434. http://dx.doi.org/10.1146/annurev.neuro.31.060407.125606.

Suzuki, L., Coulon, P., Sabel-Goedknegt, E.H., Ruigrok, T.J.H., 2012. Organization of cerebral projections to identified cerebellar zones in the posterior cerebellum of the rat. J. Neurosci. *32* (32), 10854–10869. http://dx.doi.org/10.1523/JNEUROSCI.0857-12.2012.

Taki, Y., Hashizume, H., Thyreau, B., Sassa, Y., Takeuchi, H., Wu, K., et al., 2013. Linear and curvilinear correlations of brain gray matter volume and density with age using voxel-based morphometry with the Akaike information criterion in 291 healthy children. Hum. Brain Mapp. *34* (8), 1857–1871. http://dx.doi.org/10.1002/hbm.22033.

Tamnes, C.K., Walhovd, K.B., Dale, A.M., Østby, Y., Grydeland, H., Richardson, G., et al., 2013. Brain development and aging: overlapping and unique patterns of change. Neuroimage *68*, 63–74. http://dx.doi.org/10.1016/j.neuroimage.2012.11.039.

Timmann, D., Daum, I., 2010. How consistent are cognitive impairments in patients with cerebellar disorders? Behav. Neurol. *23* (1-2), 81–100. http://dx.doi.org/10.3233/BEN-2010-0271.

Tzourio-Mazoyer, N., Landeau, B., Papathanassiou, D., Crivello, F., Etard, O., Delcroix, N., et al., 2002. Automated anatomical labeling of activations in SPM using a macroscopic anatomical parcellation of the MNI MRI single-subject brain. Neuroimage *15* (1), 273–289. http://dx.doi.org/10.1006/nimg.2001.0978.

Uh, J., Merchant, T.E., Li, Y., Feng, T., Gajjar, A., Ogg, R.J., Hua, C., 2013. Differences in brainstem fiber tract response to radiation: a longitudinal diffusion tensor imaging study. Int. J. Radiat. Oncol. Biol. Phys. *86* (2), 292–297. http://dx.doi.org/10.1016/j.ijrobp.2013.01.028.

Vaquero, E., Gómez, C.M., Quintero, E.A., González-Rosa, J.J., Márquez, J., 2008. Differential prefrontal-like deficit in children after cerebellar astrocytoma and medulloblastoma tumor. Behav. Brain Funct. *4*, 18. http://dx.doi.org/10.1186/1744-9081-4-18.

Viscomi, M.T., Molinari, M., 2014. Remote neurodegeneration: multiple actors for one play. Mol. Neurobiol. . http://dx.doi.org/10.1007/s12035-013-8629-x

Walhovd, K.B., Johansen-Berg, H., Káradóttir, R.T., 2014. Unraveling the secrets of white matter: bridging the gap between cellular, animal and human imaging studies. Neuroscience *276C*, 2–13. http://dx.doi.org/10.1016/j.neuroscience.2014.06.058.

Wang, S.S.-H., Kloth, A.D., Badura, A., 2014. The cerebellum, sensitive periods, and autism. Neuron *83* (3), 518–532. http://dx.doi.org/10.1016/j.neuron.2014.07.016.

Wechsler, D., 1999. Wechsler Abbreviated Scale of Intelligence: WASI. The Psychological Corporation, San Antonio.

Wechsler, D., 1997. WAIS-III, Wechsler Adult Intelligence Scale, Third ed The Psychological Corporation, San Antonio.

Westlye, L.T., Grydeland, H., Walhovd, K.B., Fjell, A.M., 2011. Associations between regional cortical thickness and attentional networks as measured by the attention network test. Cereb. Cortex *21* (2), 345–356. http://dx.doi.org/10.1093/cercor/bhq101.

Wheeler-Kingshott, C.A.M., Cercignani, M., 2009. About "axial" and 'radial' diffusivities. Magn. Reson. Med.: Off. J. Soc. Magn. Reson. Med./Soc. Magn. Reson. Med. *61* (5), 1255–1260. http://dx.doi.org/10.1002/mrm.21965.

Wierenga, L.M., Langen, M., Oranje, B., Durston, S., 2014. Unique developmental trajectories of cortical thickness and surface area. Neuroimage *87*, 120–126. http://dx.doi.org/10.1016/j.neuroimage.2013.11.010.

Winkler, A.M., Ridgway, G.R., Webster, M.A., Smith, S.M., Nichols, T.E., 2014. Permutation inference for the general linear model. Neuroimage *92*, 381–397. http://dx.doi.org/10.1016/j.neuroimage.2014.01.060.

Yarkoni, T., Barch, D.M., Gray, J.R., Conturo, T.E., Braver, T.S., 2009. BOLD correlates of trial-by-trial reaction time variability in gray and white matter: a multi-study fMRI analysis. PloS One *4* (1), e4257. http://dx.doi.org/10.1371/journal.pone.0004257.

Yendiki, A., Koldewyn, K., Kakunoori, S., Kanwisher, N., Fischl, B., 2014. Spurious group differences due to head motion in a diffusion MRI study. Neuroimage 88, 79–90. http://dx.doi.org/10.1016/j.neuroimage.2013.11.027.

Yuan, W., McKinstry, R.C., Shimony, J.S., Altaye, M., Powell, S.K., Phillips, J.M., et al., 2013. Diffusion tensor imaging properties and neurobehavioral outcomes in children with hydrocephalus. Am. J. Neuroradiol. *34* (2), 439–445. http://dx.doi.org/10.3174/ajnr.A3218.